

RSC Advances



This is an *Accepted Manuscript*, which has been through the Royal Society of Chemistry peer review process and has been accepted for publication.

Accepted Manuscripts are published online shortly after acceptance, before technical editing, formatting and proof reading. Using this free service, authors can make their results available to the community, in citable form, before we publish the edited article. This *Accepted Manuscript* will be replaced by the edited, formatted and paginated article as soon as this is available.

You can find more information about *Accepted Manuscripts* in the [Information for Authors](#).

Please note that technical editing may introduce minor changes to the text and/or graphics, which may alter content. The journal's standard [Terms & Conditions](#) and the [Ethical guidelines](#) still apply. In no event shall the Royal Society of Chemistry be held responsible for any errors or omissions in this *Accepted Manuscript* or any consequences arising from the use of any information it contains.

Color-tunable luminescent CdTe quantum dots membranes based on bacterial cellulose (BC) and application in ion detection

Yan Ge, Shiyang Chen,* Jingxuan Yang, Biao Wang, Huaping Wang*

State Key Laboratory for Modification of Chemical Fibers and Polymer Materials,
Key Laboratory of High Performance Fibers and Products (Ministry of Education),
College of Materials Science and Engineering, Donghua University, Shanghai,
201620, PR China

Email: chensy@dhu.edu.cn, wanghp@dhu.edu.cn

Tel: +862167792950

Fax: +862167792958

Abstract: Color-tunable luminescent membranes CdTe QDs on the bacterial cellulose (BC) nanofibers were successfully fabricated by in situ synthesis in aqueous solution. No nitrogen protection and expensive reagents are needed during the preparation process. The luminescent color of CdTe/BC nanocomposite membranes with green, orange and red luminescence can be tuned easily by controlling reaction time. The prepared CdTe/BC nanocomposites were characterized by X-ray diffraction (XRD), field effect scanning electron microscopy with energy dispersive X-ray analysis (FESEM-EDX) and transmission electron microscope (TEM). Ultraviolet-visible (UV-vis), photoluminescence (PL) spectra and PL quantum efficiency (PL QE)

were used to investigate the optical properties. Moreover, we attempted to make the luminescent membranes as ion test paper. The green luminescent membranes had a good selectivity for Cu^{2+} with the detection limit of 0.016 mM and the mechanism of quenching Cu^{2+} were also explored. This work provides a simple, effective and eco-friendly method for the construction of luminescent CdTe QDs on BC membranes with high detectability for detection Cu^{2+} .

Keywords: Bacterial cellulose; Photoluminescence; Quantum dots; Nanocomposite; aqueous solution; metal ion detection

Introduction

CdTe quantum dots (QDs), also known as CdTe semiconductor nanocrystals, are under heavy investigation due to their unique optical properties such as high photostability, broad absorption, and narrow emission with peak position tunable by their sizes and bandwidth controllable to a certain degree by their size distribution.^{1,2} Compared with the conventional organic fluorophores, CdTe QDs have longer fluorescence lifetime and negligible photobleaching. They can be capped by different ligands which have potential widespread applications such as biological probes,³ photocatalyst,⁴ chemosensors⁵ and solar cells.⁶ Wet-chemical preparation, as the name suggested, synthesizing QDs in colloidal solution, was one of the most successful methods to achieve QDs with high photoluminescence quantum yields and tunable size.⁷ Wet-chemical synthesis of QDs can be generally divided into water-phase and organic-phase approaches. Compared with organic-phase approach, synthesis in

aqueous system is relatively easier, cheaper, less toxic and more eco-friendly. More importantly, the products usually show good water-solubility and biocompatibility. Due to these advantages, synthesis of QDs in water solution has attracted more and more attention. However, applications of QDs in the fields of bio-analysis, optoelectronics and photocatalyst require composition of QDs with polymers.⁸ Several works about the preparation and properties of QD/cellulose nanocomposites have been reported for their potential applications in security paper or sheets with optical signatures.^{9, 10} However, natural fibers are composed of only 55-65% cellulose where the isolation and purification of fibers are needed. Besides, the current environmental issues show a pressing need for innovative, sustainable, and recyclable materials with performance at the same level or better than conventional natural fibers.

Unlike plant-based cellulose, bacterial cellulose (BC) does not contain collateral biogenic compounds like lignin, pectin and hemicellulose requiring purification and can therefore be separated in its purest form during the extracellular synthesis process.¹¹ Compared with conventional natural cellulose, BC presents unique properties and structures such as good biocompatibility, high crystallinity, ultrafine nanosized three-dimensional fibrous network structure, highly hydrophilic characteristic and excellent mechanical strength. These characteristics make BC as a good template or matrix for the synthesis of QDs,^{12, 13} or other nanoparticles and nanowires.^{14, 15}

In this paper, we reported a convenient and economical one-pot method to

prepare luminescent CdTe/BC nanocomposites. The CdTe/BC nanocomposites were successfully fabricated by in situ method using BC as matrix. Besides, we used thioglycolic acid (TGA) as ligand which is a traditional ligand for preparing CdTe QDs and sodium tellurite was employed as the more stable Te source. No N₂ protection, special ligand or particular treatment was required. The structure and the properties of the resultant CdTe/BC nanocomposites were characterized. Besides, we tried to make a kind of metal ion test paper using the CdTe/BC nanocomposite membranes.

Experimental

Materials and methods

BC was obtained by following process: *Gluconacetobacter xylinus* (1.1812), purchased from the Institute of Microbiology, Chinese Academy of Science, was cultured with basal medium (glucose 5 wt%, yeast extract 0.5 wt%, bacto-peptone 0.5 wt%; disodium phosphate 0.2 wt%; monopotassium phosphate 0.1 wt% and citric acid 0.1 wt%) the pH was adjusted to 5.0 with NaOH. After five days of static cultivation, the BC membranes were collected, boiled in 1 wt% NaOH for 30 min in order to remove the remaining culture medium and microorganism, and then repeatedly rinsed with pure water until filtrate became neutral. The thickness of resultant BC membranes was 0.3 cm. And then, the BC membranes were cut into pieces sized 4 cm × 4 cm as substrates for the following experimental process.

TGA (99%) was purchased from Sigma-Aldrich Co. LLC. Sodium tellurite (Na₂TeO₃, 97%), sodium borohydride (NaBH₄, 96%), cadmium acetate dihydrate

($\text{Cd}(\text{CH}_3\text{COO})_2 \cdot 2\text{H}_2\text{O}$, 98%), potassium chloride, sodium chloride, calcium chloride, magnesium sulphate, zinc chloride, nickel chloride, aluminum nitrate, iron (III) chloride, copper (II) chloride were purchased from Sinopharm Chemical Reagent Co. Ltd. All chemicals were used directly without any further treatment. High purity water with resistivity of $18.2 \text{ M}\Omega \cdot \text{cm}$ was used in the whole experimental process.

XRD patterns were obtained in a Rigaku D/max-2000 X-ray diffractometer with the Cu K α radiation at a scanning rate of $2^\circ/\text{s}$. The morphologies and elemental composition of the samples were characterized using S-4800 FESEM-EDX and JEM-2100F TEM. Prior to FESEM analysis, the samples were cut into small pieces and coated with a thin layer of evaporated gold. Prior to TEM analysis, the QDs on BC nanofibers were dispersed into pure water by ultrasonic dispersion. UV-vis spectra were measured on Lambda 35 spectrophotometer (PerkinElmer Inc.). Photoluminescence (PL) spectra were measured on Quant Master 40 spectro-fluorometer (Photon Technology International Inc.), and PL QE was measured on the same spectrofluorometer with an integrating sphere accessory. The samples were excited by ultraviolet light of same wavelength (370 nm). XPS experiment was carried out on a RBD upgraded PHI-5000C ESCA system (PerkinElmer Inc)

Fabrication of CdTe/BC nanocomposites

In a typical fabrication, the molar ratio of Cd^{2+} : TGA : Te^{2-} was 1.0 : 1.0 : 0.2, pH was 11.5. Firstly, 0.1 mmol $\text{Cd}(\text{CH}_3\text{COO})_2 \cdot 2\text{H}_2\text{O}$ was dissolved in 10 mL pure water. Then 7 μL TGA was added and pH was adjusted to 11.5 with 1M NaOH solution. The purified BC membranes were immersed into a three-necked flask containing the 10

mL Cd-TGA solution, standing for 1 h in order to reach the adsorption equilibrium. Then, 0.02 mmol Na_2TeO_3 which was dissolved in 35 mL pure water was injected slowly into the above mixture. After shaking gently for 5 min, 0.04 g NaBH_4 was dissolved in 5 mL pure water and injected slowly into the mixture, shaking for 5 min to be dispersed and produced Te^{2-} . Then, the flask was attached to a condenser and refluxed at 100 °C with stirring under open-air system for a specific period of time. Finally, the membranes were rinsed with pure water for several times and dried at room temperature. Through controlling the reaction time (0.5 h, 2 h and 13 h, respectively), the CdTe/BC nanocomposites with different PL emission (green, orange and red) can be obtained.

The selective and sensitive detection of metal ion

For the selective experiment, we prepared K^+ , Na^+ , Ca^{2+} , Mg^{2+} , Zn^{2+} , Ni^{2+} , Al^{3+} , Fe^{3+} and Cu^{2+} stock solution with concentration of 1 mM. Then we dipped the metal ion solutions onto the nanocomposite membranes. After 5 min, we measured the PL intensity of the membranes (F) and compared with the PL intensity of the membranes without metal ion (F_0) to find out the specific metal ion. To investigate the detectability of as-prepared nanocomposite membranes, various Cu^{2+} concentrations were prepared by serial dilution from Cu^{2+} stock solution. Subsequently, the PL intensity of these membranes was measured.

Result and discussion

Synthesis of CdTe/BC nanocomposites

BC has a porous structure with a large number of hydroxyl groups on the surface of

its nano fibres. Due to its unique structure, TGA capped Cd^{2+} can easily penetrate into the inner space of BC. During the soaking of BC in Cd-TGA solution, Cd^{2+} ions are firstly anchored onto BC nanofibers through the hydrogen bonds between the carboxylate anion of TGA and the hydroxyl groups of BC.¹⁶ After Na_2TeO_3 and NaBH_4 added, the Te^{4+} are reduced to Te^{2-} , and CdTe are formed with the strong interaction between Cd^{2+} and Te^{2-} , as illustrated in Fig. 1. It should be noticed that NaBH_4 plays two roles in this reaction. The first is leading to a fast reduction of Te^{4+} to Te^{2+} to supply the rapid nucleation of QDs, and the second is supplying a protective surrounding to avoid the oxidation of Te^{2-} during QD growth even without N_2 protection.¹⁷ So an excess of NaBH_4 is adopted.

XRD analysis

The crystallographic nature of the QDs in BC was further investigated by XRD to confirm the formation of CdTe QDs. The XRD of pure BC and CdTe/BC nanocomposites are shown in Fig. 2. Compared with XRD of pure BC, the broad diffraction peaks at 14.4° , 16.6° and 22.7° in the CdTe/BC nanocomposites are assigned to the crystallographic plane of $(1 \bar{1} 0)$, $(1 1 0)$ and $(2 0 0)$ reflection of BC.¹⁸ According to the reference¹⁹ and the standard card of CdTe (JCPDS Card No.15-0770), the CdTe QDs should exhibit three diffraction pattern at about 24° (111), 39° (2 2 0) and 47° (3 1 1). However, we only observed two characteristic diffraction pattern at 41.4° (2 2 0) and 47.4° (3 1 1) which slightly moved toward higher angles compared with the data in the standard card. The characteristic (111) reflection for CdTe QDs may merge into the BC (2 0 0) reflection. The shifting of the other

diffraction pattern indicated a CdS shell formed on the surface of the CdTe QDs. It is because a small amount of S^{2-} which comes from the continuous decomposition of TGA can form CdS with excessive Cd^{2+} during the reaction. The resultant CdS can cap on the surface of CdTe QDs, and as a result, the surface defects of QDs were improved and aggregation and oxidation of QDs were blocked. Similar changes in diffraction patterns were also observed during the growth of a ZnS shell on a CdSe core by Dabbousi et al.²⁰ The diffraction peak at 28.0° corresponding to the (1 1 1) crystal planes of CdS (JCPDS Card, No. 21-0829) also confirmed that CdS existed in the nanocomposites.

The crystallinity degree (CrI %) of pure BC and CdTe/BC nanocomposites was also determined by XRD analysis. The crystallinity degree of pure BC was 81.4%, in a good agreement with the literature values.²¹ However, the crystallinity degree of CdTe/BC nanocomposites were 67.8%, 66.7% and 65.1%, respectively, corresponding to 0.5 h, 2 h and 13 h, which were lower than pure BC and showed a decreasing tendency as the reaction time increased. The decreasing of crystallinity of CdTe/BC nanocomposites can probably be explained as follows: with the growth of CdTe QDs in situ on the nanofibres of BC, the hydrogen bonds among BC nanofibres were gradually damaged, leading to the increase of amorphous areas. The mechanical properties were also investigated by the tensile test. The tensile stress–strain behaviors of the pure BC and CdTe/BC nanocomposite (13 h) are shown in Fig S1 (Supporting Information). It is concluded that the tensile strength and Young's modulus of the nanocomposite have not decreased obviously indicating a good chemical stability.

FESEM-EDX and TEM analysis

The morphology of pure BC and the CdTe/BC nanocomposite was studied using FESEM and TEM shown in Fig. 3. From the representative image of CdTe/BC nanocomposite (13 h) in Fig. 3b, we can see that the porous network structure of CdTe/BC nanocomposite is intact. This exquisite structure gives a good tunnel for Cd²⁺ adsorption and results in homogeneous distribution of Cd²⁺ on BC nanofibers.²² TEM was further used to observe the size and the distribution of CdTe QDs on BC nanofibres by sonicating the CdTe/BC nanocomposite (13 h). From the images shown in Fig. 3c and Fig. 3d, we can observe that the size of the nanoparticles is about 6 nm and the nanoparticles homogeneously distributed on the surface of the nanofibers. Electron dispersive X-ray spectroscopy (EDX) was also used in conjunction with the FESEM to determine elemental composition of the nanocomposite. The ratio of detected elements was in agreement with the fabrication which is shown in Fig. S2 and Table S1 (Supporting Information).

Optical properties

The UV–vis absorption spectra of pure BC and CdTe/BC nanocomposites were performed shown in Fig. 4. From the Figure, no absorption band is observed in pure BC spectrum. In contrast, a wide absorption band can be seen on the spectra of CdTe/BC nanocomposites. With the prolonging of reaction time, the UV-vis absorption band of the CdTe/BC nanocomposites shifted to longer wavelengths because of increasing size of the CdTe nanoparticles as a consequence of the quantum confinement effect.²³ The size of the QDs can be controlled by changing the reaction

time and easily monitored by absorption spectra and PL spectra.

The PL spectra of CdTe/BC nanocomposites with an excitation wavelength at 370 nm are shown in Fig. 5. The CdTe/BC nanocomposites reacting for 0.5 h, 2 h and 13 h, respectively, exhibit a significant emission peak at 551 nm, 587 nm and 625 nm, corresponding to green, orange and red fluorescence, respectively. With prolonging the reaction time, the PL spectra of the CdTe/BC nanocomposites shifted to longer wavelengths due to quantum confinement effect as well, which had a similar tendency with UV-vis spectra. The images of CdTe/BC nanocomposites under room light conditions (top) and excited under ultraviolet (bottom) are also displayed in Fig. 6. Obviously, the CdTe/BC nanocomposites can emit fluorescence with high brightness and homogeneity. It is clear that the color of CdTe/BC nanocomposites can be tuned from green to orange and red easily by controlling reaction time.

The PL QE of CdTe/BC nanocomposites with different reaction time was measured with an integrating sphere accessory. The highest PL QE of as-prepared nanocomposites (reacting for 2 h) can reach 38.0%, and the PL QE of the other two nanocomposites was 7.8% (reacting for 0.5 h) and 24.7% (reacting for 13 h), respectively. It can be seen that the PL QE first increase then decrease with prolonging reaction time, which had a similar tendency to PL intensity.

During the early stage of CdTe QDs growth, which was the nucleation stage of QDs, the particles collided and combined to form a larger one with many defects because there was not enough particles to form a larger particle with regular shape. Therefore the PL intensity was low in this stage and it would gradually increase with

the QDs growth. When the QDs growth reached a certain extent, the particles started to grow by the Ostwald Ripening (OR) process.²⁴ With further prolonging the reaction time, smaller particles started to dissolve thus releasing monomers that were then used up by the larger particles, leading to broadening the size distribution and increasing the number of surface defects. Thus, with further prolonging the reaction time, the intensity of PL would decrease. The half peak width of the three PL peaks is also calculated as 44 nm, 48 nm and 50 nm, respectively. Compared with the data from CdTe QDs solution (red, 70 nm),²⁵ the half peak width of the nanocomposites is narrower, indicating a narrower size distribution of CdTe QDs growing on BC matrix.²¹ Besides, compared with CdTe QDs solution, the decrease of PL intensity of CdTe QDs with long reaction time is much lower when BC matrix exists, which decreases only about 6%.²⁵ This is because the nanofibre network structure of BC can enhance the stability of QDs growing in situ on it and prevent them from dissolution during OR process to some extent. Consequently, BC matrix can suppress the OR process of CdTe QDs growth and decrease surface defects.

CdTe/BC nanocomposite membranes in metal ion analysis

QDs have been used to detect metal ions in terms of different impacts on their fluorescence. However, conventional detection uses QDs solution, which is not convenient and intuitive sometimes, and need an instrument such as spectrofluorometer to analyze. Herein, we attempted to make the CdTe/BC nanocomposite membranes as a kind of ion test paper. We designed experiments to demonstrate the sensitivity to a certain metal ion for the as-prepared membranes. K^+ ,

Na^+ , Ca^{2+} , Mg^{2+} , Zn^{2+} , Ni^{2+} , Al^{3+} , Fe^{3+} and Cu^{2+} stock solution with concentration of 1mM were dipped onto the CdTe/BC nanocomposite membranes to detect the changes of the luminance. As a result, no obvious changes were observed for the orange and red luminescence of CdTe/BC nanocomposite membranes. This can be attributed to the different size of QDs with different reaction time. The surface of QDs plays an important role in their fundamental properties. For smaller particles, the surface atoms are chemically more active because they have fewer adjacent coordinate atoms and unsaturated sites or more dangling bonds. Thus, for larger QDs, their selectivity and sensitivity is relatively lower.²⁶ For the green luminescent CdTe/BC nanocomposite membranes, a good selectivity for Cu^{2+} was observed. As shown in Fig. 7a, ions other than Cu^{2+} did not cause significant changes in the PL intensity of luminescent membranes. Fig. 7b shows the image of green CdTe/BC membrane excited at 370 nm before and after Cu^{2+} treatment. Therefore, the green luminescent membrane has a good selectivity for Cu^{2+} . A series of Cu^{2+} solutions of various concentrations were prepared to preliminarily investigate the detectability of the green luminescent membranes shown in Fig. 8. It can be seen that the concentration of Cu^{2+} was reduced to 0.01 mM, an obvious decrease of PL intensity can still be observed, which implied the green luminescent membrane was sensitive to Cu^{2+} to some extent. The limit of detection, as described by the International Union of Pure and Applied Chemistry (IUPAC) ($\text{LOD} = 3 \times \text{Standard deviation/Slope}$), was calculated to be 0.016 mM. Also, with the increase of Cu^{2+} concentration, the PL intensity decreased highly and no obvious change in the shape of the PL spectrum accompanied quenching, except a

slight red-shift at higher Cu^{2+} concentration.

XPS were carried out to investigate the mechanism of quenching with Cu^{2+} . Fig. 9 shows the high-resolution spectra of Cu (2p) region of the sample after Cu^{2+} treatment (1mM) (The whole XPS spectrum shown in Fig. S3 in Supporting Information). After modified by AugerScan software, two positions (931.7, 951.4) belonged to Cu^+ ($2p_{3/2}$, $2p_{1/2}$) and two positions (932.8, 953.0) are belonged to Cu^{2+} ($2p_{3/2}$, $2p_{1/2}$) are obviously observed, respectively. It is because that after treatment with Cu^{2+} , the incorporation of Cu^{2+} into the quantum dot results in the surface defects of QDs, leading to a nonradiative recombination of the excitons and fluorescence quenching, which can be described as the mechanism of cation exchange. With the concentration of Cu^{2+} increased, the conduction band electrons of QDs induced the reduction of Cu^{2+} to Cu^+ . More Cu^+ ions will be formed and replace the Cd in the surface when the concentration of Cu^{2+} increased. Cu^+ effectively quenches the luminescence of CdTe QDs by facilitating nonradiative recombination of excited electrons (e^-) in the conduction band and holes (h^+) in the valence band. Meanwhile, come of Cu^+ can replace the Cd in the surface of CdTe QDs, which has a lower energy level than that of pure CdTe QDs on BC matrix.²⁷⁻²⁹ Thus, a red-shift of the PL spectra of luminescent membranes can be observed. This may explain the selective response of green luminescent membranes toward Cu^{2+} ions. Furthermore, the reaction is rapid and specific. In general, it guarantees the effective detection to Cu^{2+} .

Conclusions

In conclusion, the color-tunable CdTe/BC nanocomposite membranes with high

photoluminescence intensity were successfully synthesized in situ using BC as the matrix. The result from the XRD analysis shows that the CdTe nanoparticles are capped with CdS, which can improve the quality and properties of CdTe QDs, indicating that BC fibers can induce the growth of nanocrystals. It is found that the CdTe nanoparticles were homogeneously dispersed on the BC nanofibre. The nanocomposites integrate the photoluminescence properties of CdTe QDs and the green luminescent membranes had a good selectivity for Cu^{2+} which guarantees the possibility of further study on the membrane used as a kind of Cu^{2+} test paper, luminescent membranes and sensors.

Acknowledgements

This work was financially supported by Program of Introducing Talents of Discipline to Universities (B07024), Shanghai Leading Academic Discipline Project (B603), The National Natural Science Foundation of China (51273043), Project of the Action on Scientists and Engineers to Serve Enterprises (2009GJE20016).

References

1. W. J. Parak, T. Pellegrino and C. Plank, *Nanotechnology*, 2005, **16**, R9–R25.
2. D. Gerion, W. J. Parak, S. C. Williams, D. Zanchet, C. M. Micheel and A. P. Alivisatos, *J. Am. Chem. Soc.*, 2002, **124**, 7070–7074.
3. A. M. Smith, S. Dave, S. Nie, L. True and X. Gao, *Expert Rev. Mol. Diagn.*, 2006, **6**, 231–244.
4. H. Li, X. He, Z. Kang, H. Huang, Y. Liu, J. Liu, S. Lian, C. H. Tsang, X. Yang

- and S. T. Lee, *Angewandte Chemie*, 2010, **49**, 4430–4434.
5. L. Cui, X.-P. He and G.-R. Chen, *RSC Adv.*, 2015, **5**, 26644–26653.
 6. I. Robel, M. Kuno and P. V. Kamat, *J. Am. Chem. Soc.*, 2007, **129**, 4136–4137.
 7. C. B. Murray, D. J. Norris and M. G. Bawendi, *J. Am. Chem. Soc.*, 1993, **115**, 8706–8715.
 8. C. Chang, J. Peng, L. Zhang and D.-W. Pang, *J. Mater. Chem.*, 2009, **19**, 7771–7776.
 9. T. Abitbol and D. G. Gray, *Cellulose*, 2008, **16**, 319–326.
 10. T. Niu, Y. Gu and J. Huang, *J. Mater. Chem.*, 2011, **21**, 651–656.
 11. K. Gelin, A. Bodin, P. Gatenholm, A. Mihranyan, K. Edwards and M. Strømme, *Polymer*, 2007, **48**, 7623–7631.
 12. Z. Yang, S. Chen, W. Hu, N. Yin, W. Zhang, C. Xiang and H. Wang, *Carbohydr. Polym.*, 2012, **88**, 173–178.
 13. J. Yang, J. Yu, J. Fan, D. Sun, W. Tang and X. Yang, *J. Hazard. Mater.*, 2011, **189**, 377–383.
 14. W. Hu, S. Chen, X. Li, S. Shi, W. Shen, X. Zhang and H. Wang, *Mat. Sci. Eng. C-Mater.*, 2009, **29**, 1216–1219.
 15. W. Hu, S. Chen, B. Zhou and H. Wang, *Mat. Sci. Eng. B-Solid.*, 2010, **170**, 88–92.
 16. R. Martínez-Mañez and F. Sancenón, *Coordin. Chem. Rev.*, 2006, **250**, 3081–3093.
 17. E. Ying, D. Li, S. Guo, S. Dong and J. Wang, *PLoS one*, 2008, **3**, e2222.

18. C. Tokoh, K. Takabe, M. Fujita and H. Saiki, *Cellulose*, 1998, **5**, 249–261.
19. M. Kumar and S. Kumar, *RSC Adv.*, 2015, **5**, 1262–1267.
20. B. O. Dabbousi, J. Rodriguez-Viejo, F. V. Mikulec, J. R. Heine, H. Mattoussi, R. Ober, K. F. Jensen and M. G. Bawendi, *J. Phys. Chem. B*, 1997, **101**, 9463–9475.
21. B. V. Mohite and S. V. Patil, *Carbohydr. Polym.*, 2014, **106**, 132–141.
22. X. Li, S. Chen, W. Hu, S. Shi, W. Shen, X. Zhang and H. Wang, *Carbohydr. Polym.*, 2009, **76**, 509–512.
23. H. Mattoussi, L. H. Radzilowski, B. O. Dabbousi, E. L. Thomas, M. G. Bawendi and M. F. Rubner, *J. Appl. Phys.*, 1998, **83**, 7965–7974.
24. M. O. M. Piepenbrock, T. Stirner, M. O'Neill and S. M. Kelly, *J. Am. Chem. Soc.*, 2007, **129**, 7674–7679.
25. S. Wu, J. Dou, J. Zhang and S. Zhang, *J. Mater. Chem.*, 2012, **22**, 14573–14578.
26. W. Zhong, J. Liang and J. Yu, *Spectrochim. Acta A*, 2009, **74**, 603–606.
27. A. Wang, L. Fu, T. Rao, W. Cai, M. F. Yuen and J. Zhong, *Opt. Mater.*, 2015, **42**, 548–552.
28. A. V. Isarov and J. Chrysochoos, *Langmuir*, 1997, **13**, 3142–3149.
29. Y. Chen and Z. Rosenzweig, *Anal. Chem.*, 2002, **74**, 5132–5138.

Figure captions

Fig. 1 Schematic formation process of CdTe nanoparticles onto BC nanofibers.

Fig. 2 XRD patterns of pure BC and CdTe/BC nanocomposites with different reaction time.

Fig. 3 FESEM images of (a) pure BC, (b) CdTe/BC nanocomposite (13 h) and TEM images of (c, d) CdTe QDs (13 h).

Fig. 4 The UV-vis spectra of pure BC and CdTe/BC nanocomposite with different reaction time.

Fig. 5 The PL spectra of pure BC and CdTe/BC nanocomposites with different reaction time (excitation wavelength at 370 nm).

Fig. 6 The image of CdTe/BC nanocomposite membranes with different reaction time (left) 0.5 h; (middle) 2 h; (right) 13 h under ambient condition (top) and after ultraviolet excitation at 370 nm (bottom).

Fig. 7 (a) Relative PL intensity (F/F_0) of green luminescent membranes with different metal ions (1mM), (b) The image of CdTe/BC nanocomposite (0.5 h) excitation at 370 nm before and after Cu^{2+} treatment.

Fig. 8 The PL intensity of green luminescent membranes with various concentrations of Cu^{2+} .

Fig. 9 XPS spectra for the Cu^+ (2p) and Cu^{2+} (2p) region of green luminescent membrane after treatment with Cu^{2+} (1mM)

Fig. 1

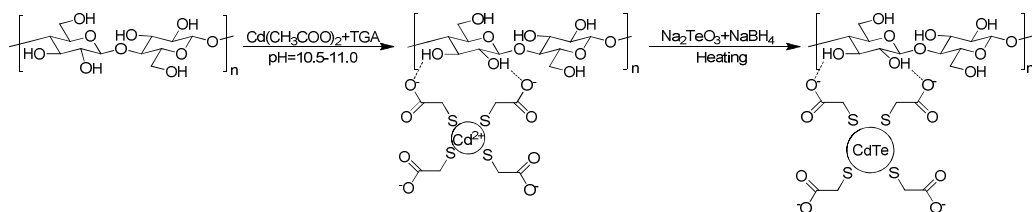


Fig. 2

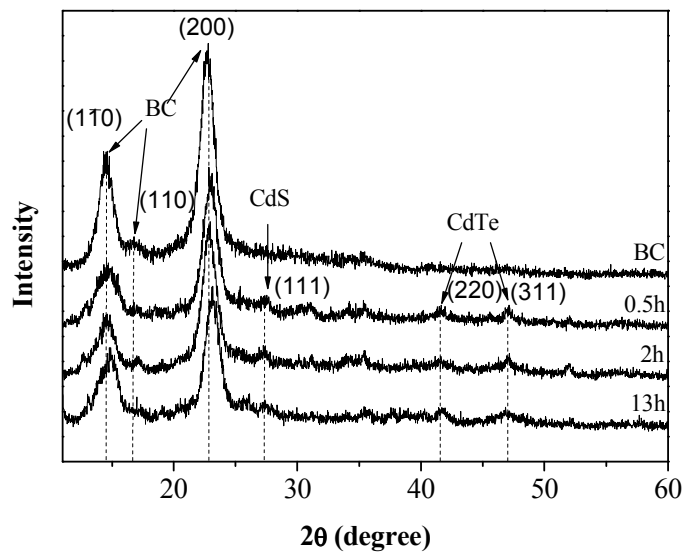


Fig. 3

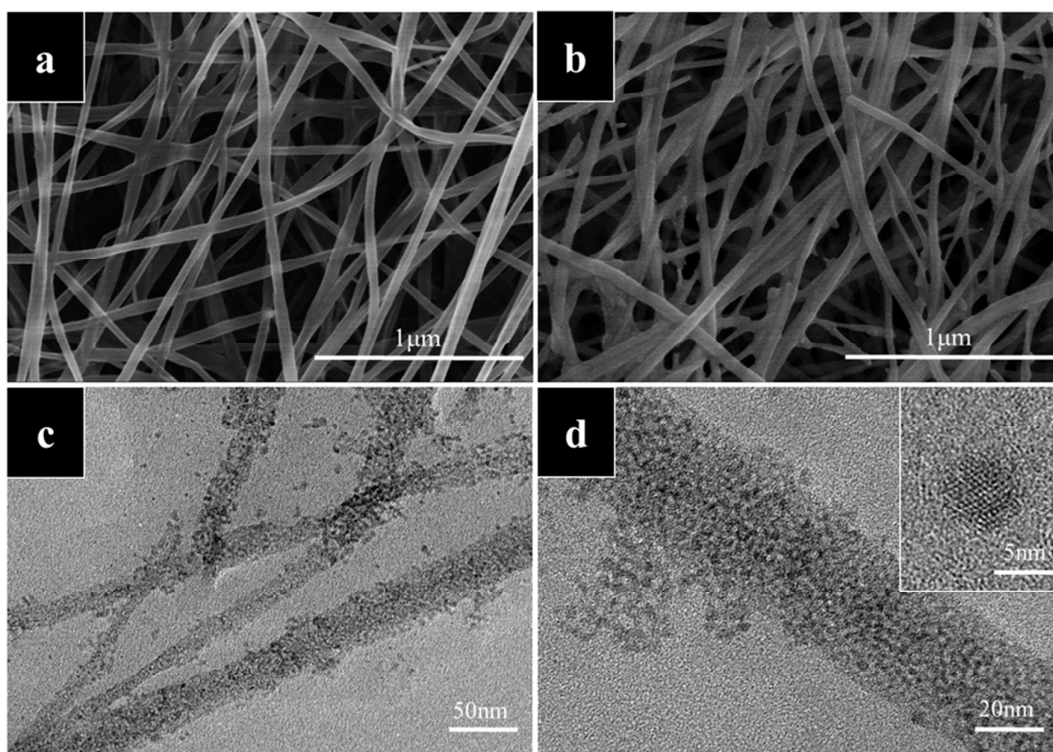


Fig. 4

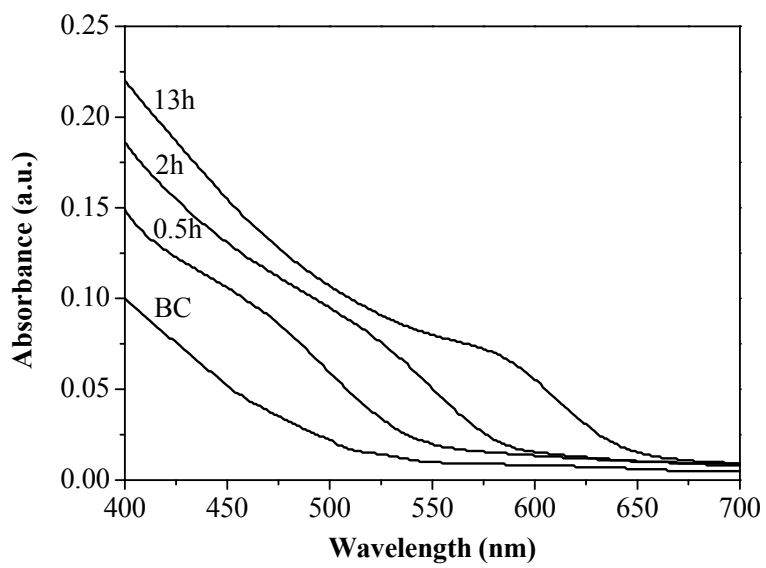


Fig. 5

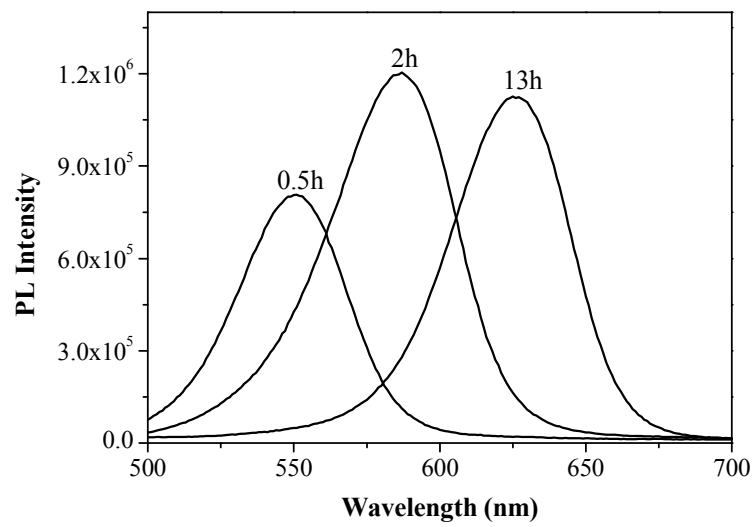


Fig. 6

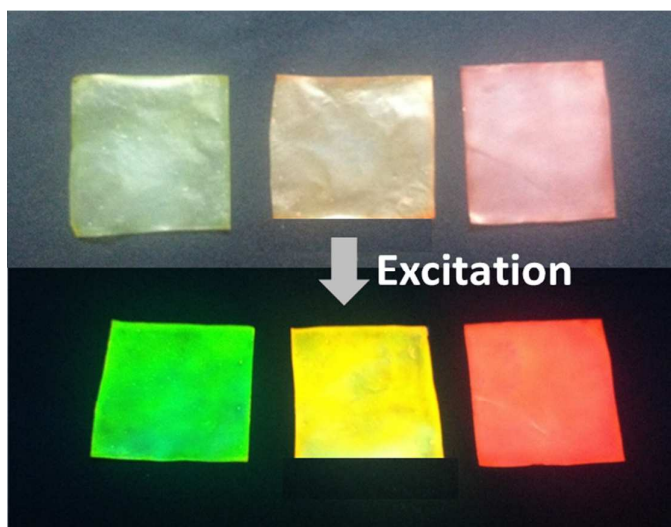
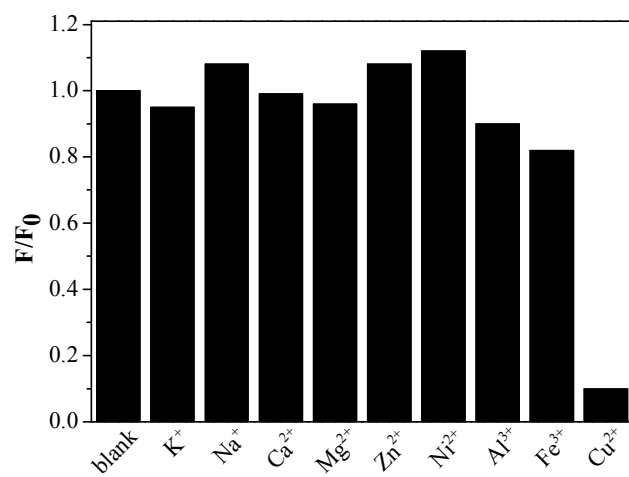
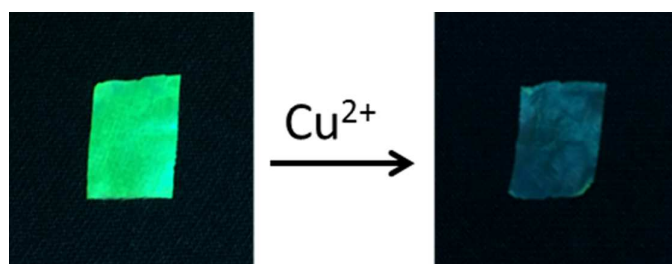


Fig. 7



(a)



(b)

Fig. 8

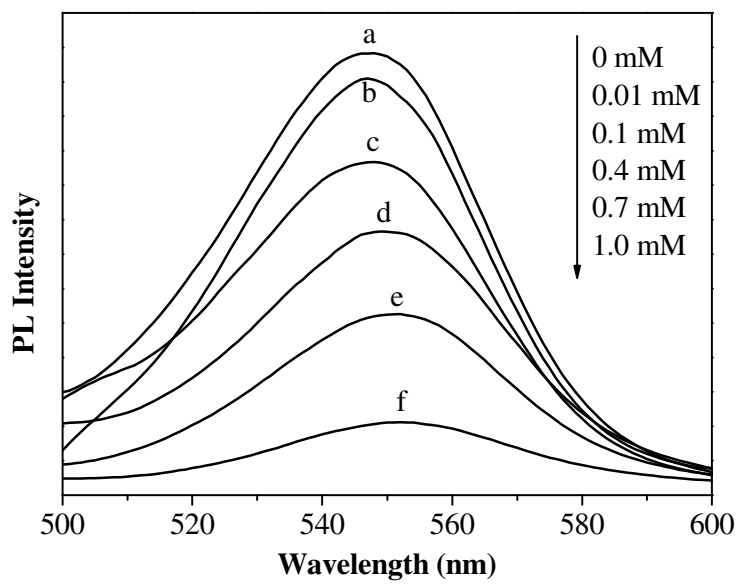


Fig. 9

